SURFACE ROUGHNESS AND TENSILE PROPERTIES OF COPPER-CARBON-POLYAMIDE COMPOSITE BY SELECTIVE LASER SINTERING

W.K.C Wolf [1, 2], I. Yadroitsava [1] & I. Yadroitsev [1]

[1]Department of Mechanical and Mechatronics Engineering,
Central University of Technology, Free State (CUT), Bloemfontein 9300, South Africa
wwolf@cut.ac.za

[2]Centre for Rapid Prototyping and Manufacturing, Central University of Technology, Free State, South Africa

ABSTRACT

Medical development in additive manufacturing (AM) has overcome multiple challenges in material functionality. Polymer materials are increasingly used in the manufacture of medical device components by AM. The presented investigations are concerned with the manufacturing and analysis of samples produced by selective laser sintering (SLS). Test samples were manufactured from conductive polyamide-12 (CB/PA12) and mixture of CB/PA12 with 10 wt.% pure Cu powder. Tensile properties and fractures as well as surface roughness of manufactured samples were evaluated during the study.

1. INTRODUCTION

Selective laser sintering (SLS) is a type of additive manufacturing (AM) wherein a bed of powder polymer or elastomer is targeted sintered by laser, with subsequent solidification of the powder layer. A laser sintering (LS) machine usually is composed of the powder reserve chamber, the printing chamber, and extraction chamber. Printing chambers are initially heated up to a certain temperature just below the melting point of the material to be sintered. The properties of SLS parts rely on various inputs of LS machine process parameters. The key contributing factors that influence the process are preheating temperature of the powder bed, laser power, scan speed, scan spacing, layer thickness and chamber temperature.

One of the advantages of LS is the possibility to produce in-situ sintered materials from a powder mixture [1-4]. Fillers were introduced and were readily accepted because they are easy to incorporate into plastics and offer many possibilities for product improvement and differentiation. Fillers are an extremely diverse group of materials. They can be minerals, metals, ceramics, bio-based, gases, liquids, or even other polymers. The properties required of fillers for plastics include colour, strength, electrical and thermal conductivity. Addition of a filler changes many properties at once, so successful formulation depends on an understanding of structure–property relationships. It can change colour, increase the hardness and wear resistance of polymers, and furthermore improve other specific properties such as flame retardancy thus making the product more functional.

Medical development in additive manufacturing (AM) has overcome multiple challenges in material functionality. New classes of modified biomaterials used in design and manufacturing of medical devices include metals, ceramics, glass and polymers. Polymer materials are increasingly used in the manufacture of medical device components because of the wide range of desirable properties they offer including biocompatibility, cost effectiveness, design flexibility, and balanced mechanical properties. Polyamide 12 (PA12) covers 95% of SLS powders and is used in almost all LS commercial systems. Polyamide-12 is a proven SLS plastic material for biomedical applications that is used for production of functional prototypes and end-use components. PA powders can be relatively easily reinforced with other materials in order to further improve their mechanical and thermal properties. PA coated copper powder (Cu-PA12) is also available for the production of plastic-metal composite injection moulding tools. These moulds can be used for fabrication of a limited number of pre-production parts in the same material and manufacturing process as the final production parts. PA is characterised by mechanical properties ideally suited for medical tubing, where push ability and torque performance are primary considerations. Therefore, it has been extensively used for medical applications such as catheters, surgical planning, surgical guides and blood sets.

However, many polymer surfaces are easily colonised by microorganisms, particularly in-house devices such as urinary Foley tubes that pass through the skin or body-contacting fluids and tissues especially when they are used for extended periods [4-6]. The surfaces of these devices provide the opportunity for the formation of biofilms that can facilitate the growth of infection and fever causing microorganisms. Growth of microorganisms can also cause staining, discoloration, odour, and reduction of performance and material properties. The increasing awareness of hospital acquired antibiotic resistant infections has led to increased use of alternative antimicrobials in medical devices, equipment housings and hygienic surface applications.

Anti-bacterial properties in 3D printed parts have been intensively investigated in recent years due to the wide range of applications including bone tissue engineering regeneration to treat bone fractures, the fabrication of biomedical devices that are able to prevent biofilm formation, the fabrication of wound dressing, or the fabrication of scaffolds [1]. In biomedical engineering, the main focus has been on the development of biopolymeric materials for tissue and scaffold generation with improved flexibility, strength, and patient compatibility in order to prevent implant rejection and toxicity. In order to provide antibacterial activity to a 3D

printed part, different alternative strategies can be employed, which include among others the use of antimicrobial polymeric materials, the incorporation and release of antimicrobial agents, or introducing antibacterial functionality through the surface modification of the part [4-6].

Polyamides represent an important class of biomaterial as it may be possible to exploit their hydrophilic nature to increase the release of metal ions at a concentration level that is capable of ensuring antibacterial characteristics. Since pure copper (Cu) has anti-bacterial properties, polyamide-copper anti-bacterial composites will address the issues of reducing the total number of infections in the medical industry. Literature shows that significant research has been done on understanding which polymer characteristics could impact the efficacy of the polymer/antimicrobial composite [7-9]. Chemical structure, morphology and polarity could influence the rate of metal ion release.

Direct incorporation of metallic antimicrobial agents into the polymer matrix is a better alternative to coating techniques for the development of antimicrobial polymers. The advantage of this approach is that the processing parameters, as well as the polymer technologies involved in the device manufacture, do not require significant modification. As a result, the cost of metallic antimicrobial composites prepared using this method will render long term antimicrobial efficacy when compared to coating techniques.

2. MATERIALS AND METHODS

A Sintratec S1 (Switzerland) laser sintering system was used to produce specimens for this study. This system is equipped with a 2.3 W blue diode (445 nm) laser of 250 μm spot size and it has a 0.13 m x 0.13 m x 0.18 m print size which allows for building small prototypes and end-use consumer products from polymer materials.

As is known, plastics absorb laser radiation in the ultraviolet and infrared regions, so for transparent plastics such as PA12, CO_2 or excimer lasers are used (Figure 1). Diode lasers are light, have a long lifespan and are reliable which make them well suited for use in additive manufacturing. These lasers cover a wide spectrum of wavelength from 405 to 1080 nm.

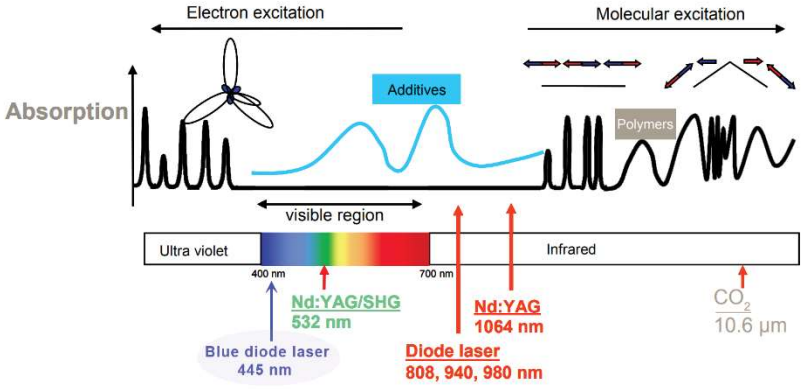

Figure 1: Absorption of laser radiation of plastics at different wavelength (adapted from [12])

To make transparent plastics "sensitive" to the generated wavelength and to absorb energy from the laser beam, different fillers and colorants such as TiO2 or carbon can be added to the plastic. Varying the concentration of these compounds allows for absorption and scattering in such plastics to be managed [10-12].

Black PA12/CB powder from Sintratec was used in the current research. PA12 powder is transparent for the diode laser used in the Sintratec S1 system, so carbon is added to PA12 power by Sintratec to improve absorption of the laser beam energy in the blue region. Magnification of the powder show that some of the particles are covered in carbon (Figure 2a, b). The semi crystalline thermoplastic polymer powder is anthracite in colour with average particle size of between 60 μm and 100 μm. It has a low molecular weight, the melting temperature is in the range of 177°C–185°C and the density is 1000 – 1150 kg/m³.

The employed Cu powder (–45 μm) (TLS Technik GmbH & Co. Spezialpulver KG) used in the study has 99.9% purity. The 10th, 50th and 90th percentiles of equivalent diameter (weighted by volume) of the powder are d_{10} =9 μm, d_{50}=22 μm and d_{90}=38 μm, respectively. The employed Cu powder was gas atomised and spherical in shape (Figure 2 c, d). The maximum size of Cu powder particles was compatible with average size of CB/PA12 powder particles.

The Cu powder and matrix material, virgin nylon (CB/PA12), were used in a weight ratio of 10/90 respectively. The Cu and PA12 were mixed in a horizontal rotating drum mixing station for 5 hours at 60 rpm to insure homogenous distribution of the powder particles. After mixing the material, it was left to dry for 12 hours at room temperature. The mixture was then sieved one time through a 150 μm sieving tool and was loaded into the SLS machine for building of specimens for mechanical testing. The material preparation was performed at room temperature.

For initial experiments, standard process parameters recommended by Sintratec for CB/PA12 powder were used (Table 1). Specimens were manufactured in different orientations as indicated in Figure 3. The dimensions of the specimen corresponded to the ASTM D638-12 standard (Type V) [13]. Tensile tests were performed with a crosshead speed of 1.5 mm/min using a MTS Criterion universal testing machine. The surface roughness of the specimens was measured using a Mitutoyo SJ-210 surface roughness tester which fulfils ISO 1997 requirements. The parameters used for the roughness measurements were as follows: six randomly selected samples were tested along the length of the tensile specimens; sampling length was 2.5 mm, transition length was 15 mm and the Gaussian filter was selected with a cut-off length λ_c=2.5 mm. The polymer blend specimens were observed under a Jeol Neoscope scanning electron microscope (SEM) to investigate the powders and fracture surface. The specimens were studied without any coating at 5-15 kV.

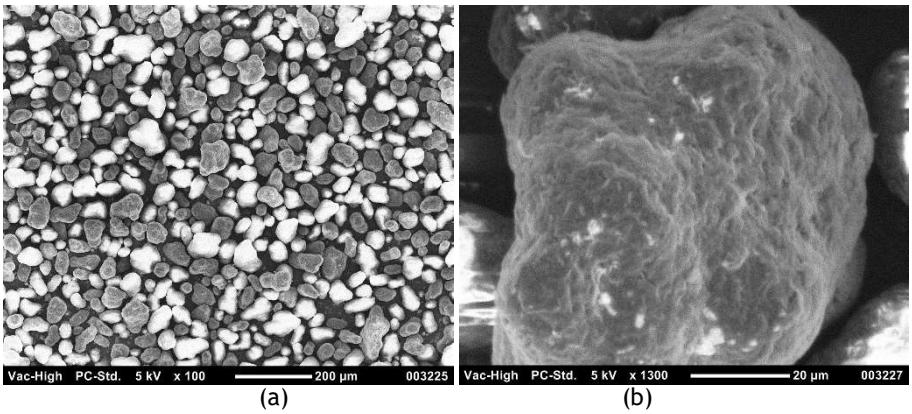

(a) (b)

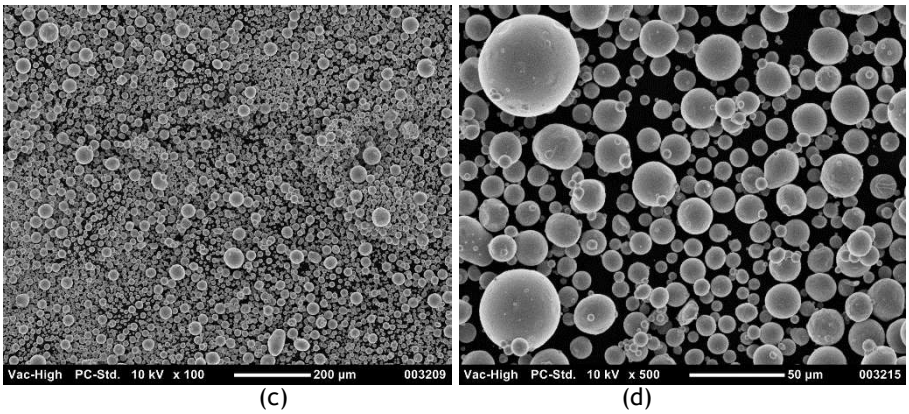

(c) (d)

Figure 2: SEM photos of CB/PA12 powder (a, b) and pure Cu powder (d, c).

Table 1. Sintratec Central build parameters recommended for CB/PA12 powder

Parameter	Value
Layer thickness, µm	100
Hatch spacing, µm	150
Laser speed, m/s	0.65
Printing surface target heating temperature, °C	150
Printing surface target printing temperature, °C	170
Chamber target heating temperature, °C	140
Chamber target printing temperature, °C	140
Pre heating time, hour	1.75

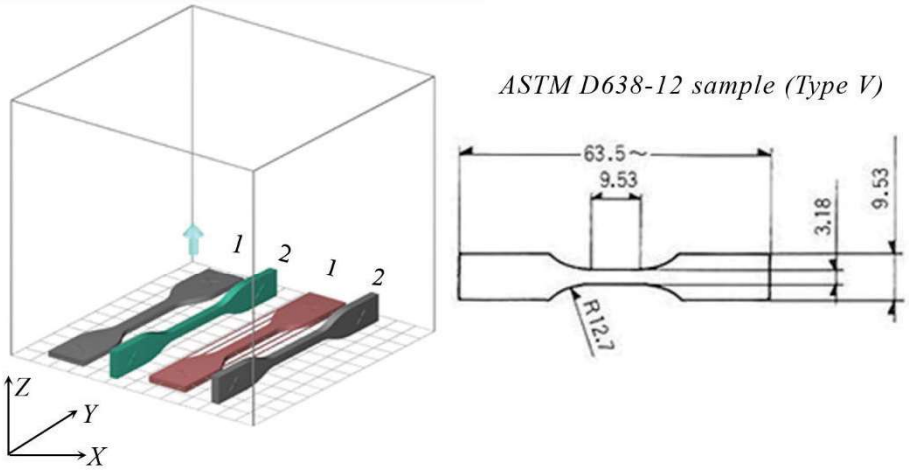

Figure 3: Specimen orientation on the build platform (left) and dimensions of samples (right).

3. RESULTS AND DISCUSSION

3.1 Surface roughness

First, the roughness of manufactured samples was analysed (Table 2 and Figure 4). All samples that were built in the YZ-direction had slightly higher roughness in comparison with XY-

samples, but from statistical t-test this difference was insignificant ($p<0.05$). The roughness measured in the YZ-directions specimens (between layers) was compaarible with in-layers roughness values of the XY-direction samples). The arithmetic mean of the absolute values of roughness profile from the mean line Ra was 9-10 μm. The root-mean-square (Rq) roughness was 11-12 μm; maximum height was about 50 μm which corresponds to a shrinkage of powder material during the sintering process. Maximum peak height Rp and maximum depth (Rv) were 25-27 μm and maximum roughness of samples Rt and Rz1max were close to the average value of powder particles (70-75 μm). The degree of asymmetry Rsk was near 0, so the amplitude distribution curves were symmetrical.

Similar to CB/PA12 samples, CB/PA12+10wt.% Cu specimens built in YZ direction were slightly rougher in comparison with XY samples. Any significant differences were found when a *t-test* ($p<0.05$) was done to compare average values of roughness of CB/PA12 samples with and without the addition of copper. Typical roughness profiles of these two types of specimens look very similar as shown in Figure 4. It must be noted that analysis of the top surfaces of samples showed homogenous distribution of Cu particles and that they were randomly distributed in the samples (Figure 5).

Table 2. Surface roughness of SLS samples

Parameter	CB/PA12		CB/PA12 + 10 wt.% Cu	
	Set 1 (N=6)	**Set 2 (N=6)**	**Set 1 (N=6)**	**Set 2 (N=6)**
	Average±S.D.	Average± S.D.	Average±S.D.	Average± S.D.
Ra, μm	9.2±0.51	9.96±0.84	8.6±0.94	9.3±0.80
Rq. μm	11.3±0.60	12.1±0.93	10.7±1.02	11.6±1.06
Rz, μm	50.5±3.3	54±3.34	49±2.9	52±5.8
Rp, μm	25.1±2.22	26.4±2.86	23.6±2.75	26.6±4.83
Rv, μm	25±±3.3	28±1.5	25±2.5	25.5±2.7
Rt, μm	69±10.8	75±10.4	66±8.9	69±9.2
Rsk	0.01±0.23	0.01±0.12	-0.06±0.28	0.05±0.44
Rz1max	65±11.1	72 ±11.4	62±9.1	64±8.8

(a)

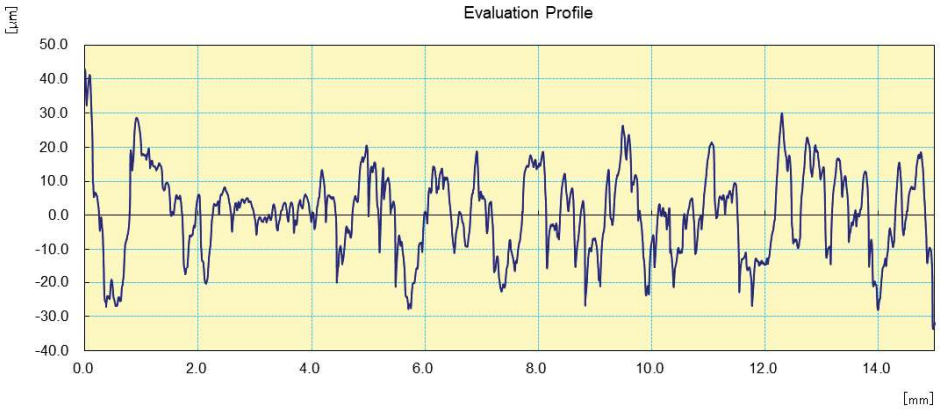

(b)

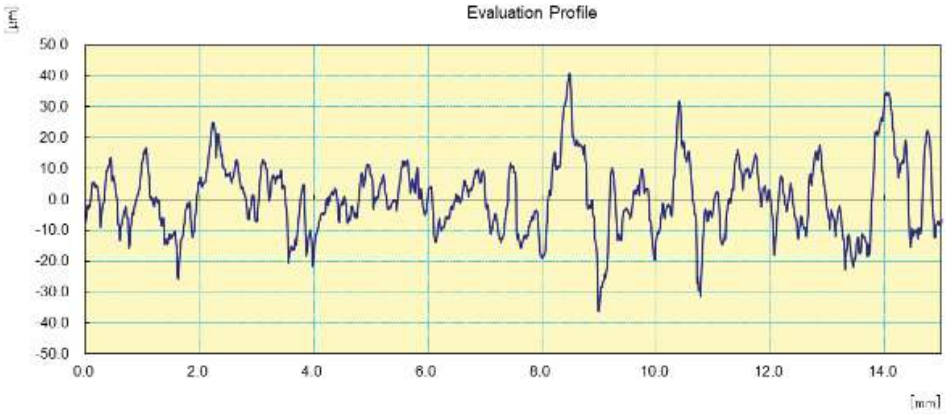

(c)

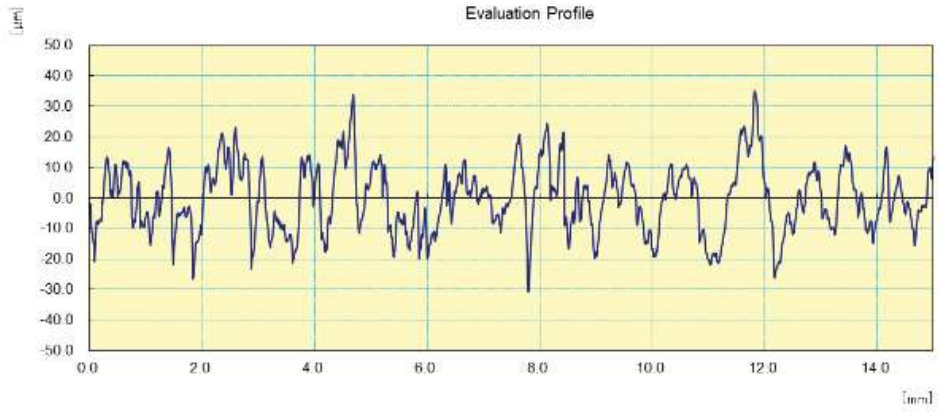

(d)

Figure 4. Roughness profiles of CB/PA12 (a, b) and CB/PA+10wt%Cu samples: sets 1 (a, c) and sets 2 (b, d).

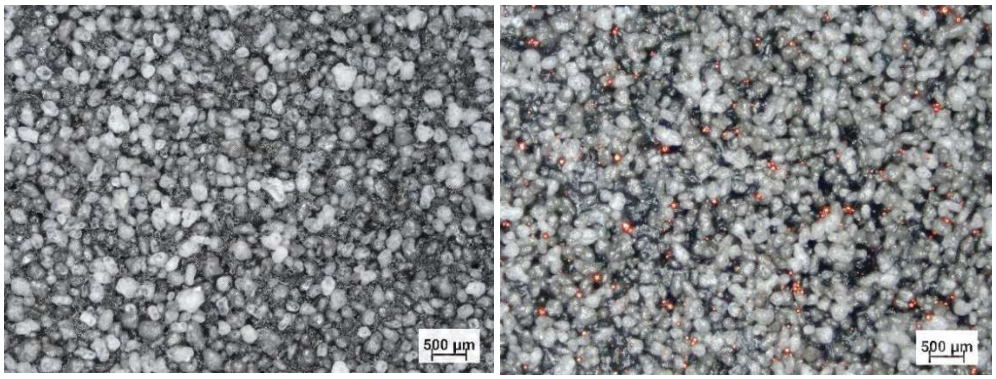

Figure 5. Top surface of CB/PA12 (left) and CB/PA+10wt.%Cu (right) samples built in the XY direction. Cu particles are visible as bright spots in the right image.

3.2 Tensile properties

Experimentally observed mechanical properties are summarized in Table 3. The tensile stress–strain curves of the as-built samples are shown in Figure 5 and are summarized in Table 2. It was found that as-built samples had no statistically significant difference (*t-test*, $p<0.05$) in yield strength, ultimate tensile strength, modulus of elasticity and elongation at break (Table 3). As can be seen from Figure 6, differences in the mechanical properties of XY-direction specimens in each series were small, the only coefficients of variation were about 30% in elongation to break. For sample, samples that were built in YZ-direction, offset yield stress and elongation varied significantly (~30% and~45% correspondingly).

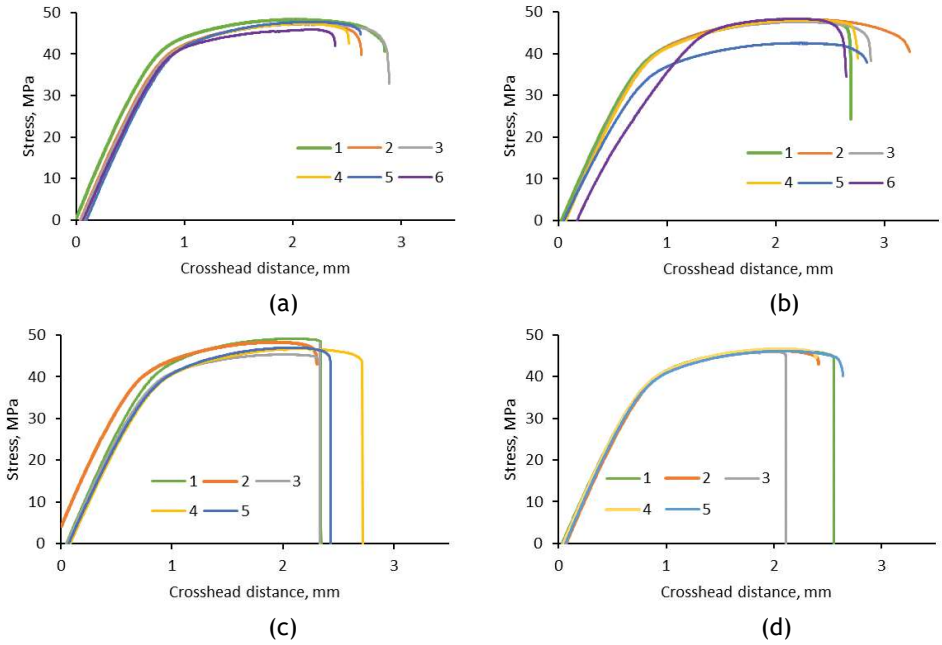

Figure 6. Stress-strain diagram of CB/PA12 samples (a, b) and CB/PA12 + 10 wt.% Cu samples (c, d) manufactured in XY (a, c) and YZ (b, d) directions.

Table 3: Tensile properties of samples manufactured in different directions

Specimens		*YTS (Offset 0.2 %), MPa*	*Elastic modulus, MPa*	*UTS, MPa*	*Elongation, %*
CB/PA12	Set 1 (XY direction), N=6	39±3.7	1772±101	47±1	10±3.1
	Coefficient of variation	9.4%	5.7%	1.7%	29.8%
	Set 2 (YZ direction), N=6	31±9.1	1821±57	48±1	13±5.7
	Coefficient of variation	29.8%	1.1%	1.1%	44.9%
CB/PA12+ 10 wt.% Cu	Set 1 (XY direction), N=5	31±3.5	1795±45	46±0.5	11±4.3
	Coefficient of variation	11.4%	2.5%	1.1%	39.3%
	Set 2 (YZ direction), N=5	33±7.4	1967±68	48±1	8±1.4
	Coefficient of variation	22.7%	3.5%	2.0%	17.7%

Samples were tested in direction parallel to the SLS layers in both cases for sets 1 and 2. These results obtained were close to the tensile results of CB/PA12 specimens with similar dimensions as was performed by Wang et al. [14] where UTS was found to be 49-51 MPa with elongation at break of 10-16%.

For CB/PA12+10wt.%Cu it was found that as-built samples had no statistically significant difference (*t-test*, $p<0.05$) in yield strength, ultimate tensile strength, modulus of elasticity and elongation at break (Table 3). As can be seen from Figure 6, differences in mechanical properties of XY-specimens (set 1) were small, only was the coefficient of variation about 30 % for elongation to break. For samples that were built in YZ-direction (set 2), offset yield stress varied significantly (~23%) and also elongation to break of about 18%. A comparison of the tensile properties of samples with 10 wt.% copper and without the addition of copper shows that only the elongation to break was different, all other parameters were very similar.

3.3 Fracture analysis

Tensile fractures of the test specimens demonstrated a complex brittle/ductile nature of the CB/PA12 specimens as shown in Figure 7a-c. Semi-sintered particles attached to the core facilitated creation of cracks. Fairly flat tearing surfaces of the fractured specimens indicate brittle fracture mode (Figure 7a), however, the fibrous and dimpled fracture surfaces (Figure 7b.c) in the core shows ductile behaviour of the sintered core material. More layers in set 2 increase the likelihood of defects so big cracks were found in different areas of the gage (Figure 7d), but fractures showed similar to set 1 complex behaviour. In Figure 7 c,e semi-sintered particles are clearly visible as isolated spheres with diameter about 40-50 μm. This can be a reason of reduced ductile behaviour of the samples produced from CB/PA12 in comparison with pure PA12 samples sintered by CO_2 laser that showed 18% elongation. These semi-sintered particles act as stress concentrators for testing and promoted brittle fracture of CB/PA 12 samples.

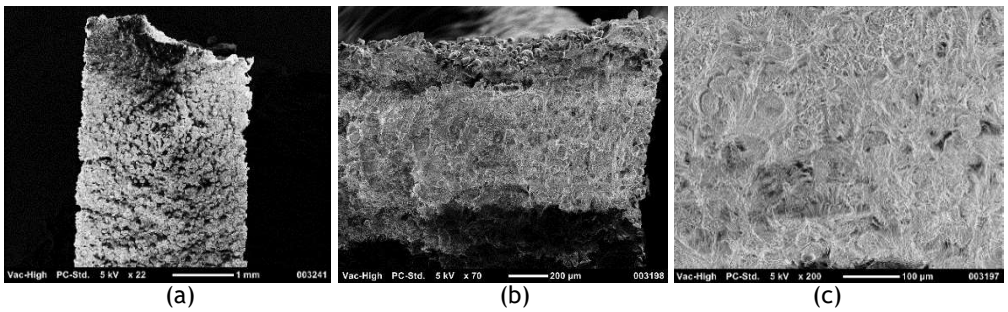

(a) (b) (c)

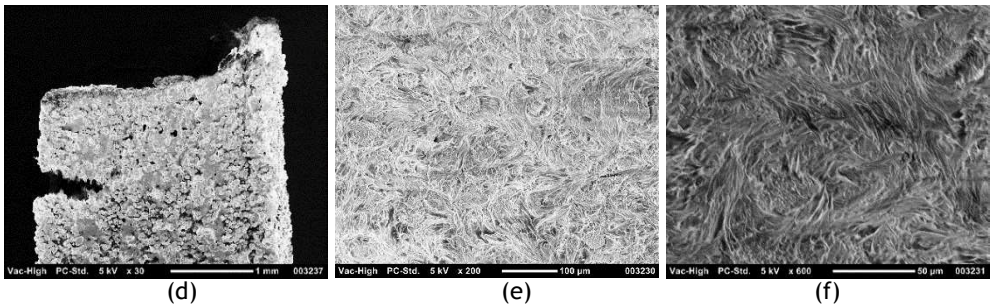

(d) (e) (f)

Figure 7. Typical fractures of CB/PA12 samples manufactured in XY (a, b, c) and YZ (d, e, f) directions.

Figure 8 presents typical fractures of composite CB/PA12+10wt.%Cu samples manufactured in the XY- and YZ-directions. These specimens had more brittle behaviour in comparison with CB-PA12 samples: lower elongation to failure and more smooth areas of the fracture surface. Poor particle-matrix adhesion for big Cu particles can cause lower ductility of these samples. Cano et al. [16] investigated tensile properties of PA12 and PA12 filled with glass. Fracture tests were performed perpendicular and parallel to the layered structure. The fracture behaviour of the composite was unaffected by the orientation in a manner similar to present study, but fracture resistance of PA12 was higher than that of the composite due to the poor adhesion of the glass beads to the matrix. In the present study, a 10 wt.%Cu addition to CB/PA12 was not a decisive factor on UTS and YS of composite samples.

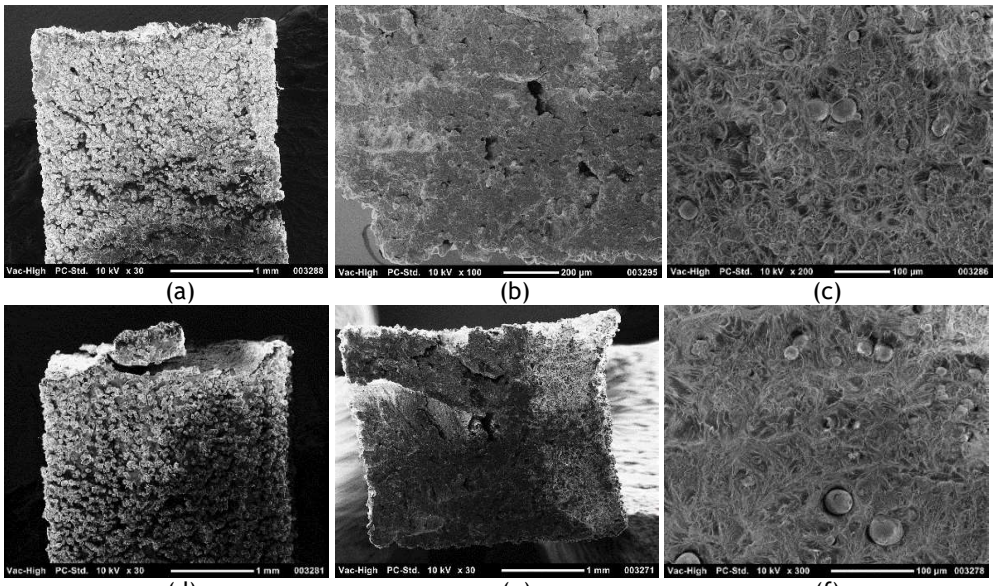

(a) (b) (c)

(d) (e) (f)

Figure 8. Typical fractures of CB/PA12+10wt.%Cu samples manufactured in XY (a, b, c) and YZ (d, e, f) directions. Round Cu powder particles are visible at high magnification (c, f).

4. CONCLUSION

This work investigated some mechanical properties of selective laser sintered in-situ copper into CB/PA12, built using the recommended process parameters from the supplier of the material. Based on the investigation conducted, the following conclusion were drawn:

- Surface roughness of all samples built in YZ-direction had slightly higher values in comparison with XY-direction samples.
- Since samples were quite small, high roughness could influenced results. Polished smooth samples are preferable for tensile testing.
- Tensile properties of samples with 10 wt.% and without copper addition show that elongation at break and fracture behaviour were different, but UTS, Elastic modulus and YS were very similar.
- Further work on optimisation of process-parameters has to be done, such as example to slightly increase build chamber temperature.
- Porosity analysis should to be done by CT scanning.

5. ACKNOWLEDGEMENTS

This work is based on research supported by the South African Research Chairs Initiative of the Department of Science and Technology and the National Research Foundation of South Africa (Grant 97994).

REFERENCES

[1] **Cama, G., Coenye, T., Dubruel, P., Dash, M., Gheysens, T., Gorzelanny, C., Misseeuw, L., Tardajo, M.G.** 2018. Chitosan functionalized poly-ε-caprolactone electrospun fibres and 3D printed scaffolds as antibacterial materials for tissue engineering applications. *Carbohydrate Polymers Journal*, 191(1), pp 127-135.

[2] **Damm C., Münstedt H., Rösch A.** 2008. The antimicrobial efficacy of polyamide6/*silver*nano and micro composites. *Materials Chemistry and Physics*, 108(1), pp 61–66.

[3] **Mazzoli, A., Moriconi, G., Pauri, G.** 2007. Characterization of an aluminum-filled polyamide powder for applications in selective laser sintering, *Materials & Design*, 28(1), pp 993-1000.

[4] Xanthos, M. 2010. Functional Fillers for Plastics, 2nd edition, Wiley-VCH Verlag Weinheim, **Germany.**

[5] **Ramstedt, M., Ribeiro, I. A. C., Bujdakova, H., Mergulhão, F. J. M., Jordao, L., Thomsen, P., Alm, M., Burmølle, M., Vladkova, T., Can, F., Reches, M., Riool, M., Barros, A., Reis, R. L., Meaurio, E., Kikhney, J., Moter, A., Zaat, S. A. J., Sjollema, J.**, 2019. Evaluating Efficacy of antimicrobial and antifouling materials for urinary tract medical devices: challenges and recommendations. Macromol. Biosci. 19, 1800384.

[6] **Darouiche, R.O., Trautner, B. W.** 2004. Catheter-associated infections pathogenesis affects prevention. *Archives of Internal Medicines, Apr 26*; 164(8), pp 842–850.

[7] **Brady, D.B., Farrell, J. B., Kealey N. C., Kennedy J.** 2017. Characterisation of polyamide 11/copper antimicrobial composites for medical device applications. *Materials Science and Engineering*, 78(1), pp 1179-1186.

[8] **Dhima, S., Negi, S., Sharma, R.K.,** 2014. Investigating the surface roughness of SLS fabricated glass-filled polyamide parts using response surface methodology. Arabian Journal of Science Engineering. 39(1). Pp 9161-9179.

[9] **Drummer, D., Greiner, S., Lanzl, L., Wudy, K.** 2019. Selective laser sintering of copper filled polyamide 12: Characterization of powder properties and process behaviour. *Polymer Composites*, 40(1), pp 1801-1809.

[10] **Aden, M., Mamuschkin V., Roesner A.,** 2013. Laser transmission welding of white thermoplastics with adapted wavelengths. *Physics Procedia*, 41(1), pp 172 – 179.

[11] **Hong, R., Leng, J., Wu J., Zhang, J., Zhao, Z.** 2019. Two-step approach based on selective laser sintering for high performance carbon black/ polyamide 12 composite with 3D segregated conductive network. Composites Part B: Engineering Journal,

[12] **Evonik Industries AG**, 2020. Polymers & Lasers. Laser Application Center. Accessed from https://www.vestamid.com/sites/lists/RE/DocumentsHP/Polymers-Lasers-EN.pdf, 16 Aug 2020.
[13] **ASTM D638-14.** Standard test method for tensile properties of plastics. *ASTM International, West Conshohocken, PA*.
[14] **Wang, Y, DiNapoli, C. M., Tofig G. A., Cunningham R. W.,** 2017. Selective laser sintering processing behavior of polyamide powders. The Plastics Technology Conference (ANTEC) Proceedings, pp. 112-116.
[15] **EOS, 2020.** Polyamide 12 for 3D Printing. https://www.eos.info/en/additive-manufacturing/3d-printing-plastic/sls-polymer-materials/polyamide-pa-12-alumide
[16] **Cano, A.J., Rodríguez J., Salazar A.** 2018. Effect of temperature on the fracture behaviour of polyamide 12 and glass filled polyamide 12 processed be selective laser sintering. Engineering Fracture Mechanics, 203(1), pp 66-80.